Performance tests of a large volume cerium tribromide (CeBr₃) scintillation detector

A.A. Naqvi [a,*], F.Z. Khiari [a], F.A. Liadi [a,b], Khateeb-ur-Rehman [a], A.A. Isab [b]

[a] Department of Physics, King Fahd University of Petroleum and Minerals Dhahran, Saudi Arabia
[b] Department of Chemistry, King Fahd University of Petroleum and Minerals Dhahran, Saudi Arabia

HIGHLIGHTS

- Pulse height tests of large diameter CeBr3 detector for low energy gamma rays using portable neutron generator based PGNAA setup.
- CeBr₃ detector has 7–8 times less total intrinsic activity than that of a LaBr₃:Ce or LaCl₃:Ce detector.
- The CeBr₃ detector has 23% smaller MDCB and 18% larger MDCCd than those of a LaBr3:Ce detector.

ABSTRACT

The response of a large cylindrical 76 mm × 76 mm (height × diameter) cerium tribromide (CeBr₃) detector was measured for prompt gamma rays. The total intrinsic activity of the CeBr₃ detector, which was measured over 0.33–3.33 MeV range, was found to be 0.022 ± 0.001 counts/s/cm³. The partial intrinsic activity (due to [227]Ac contamination), was measured over a energy range of 1.22–2.20 MeV energy, was found to be 0.007 ± 0.001 counts/s/cm³. Compared to intrinsic activities of LaBr₃:Ce and LaCl₃:Ce detectors of equivalent volume, the CeBr₃ detector has 7–8 times less total intrinsic activity.

The detector response for low energy prompt gamma rays was measured over 0.3–0.6 MeV gamma energy range using a portable neutron generator-based Prompt Gamma Neutron Activation Analysis (PGNAA) setup. The experimental yield of boron, cadmium and mercury prompt gamma-rays was measured from water samples contaminated with 0.75–2.5 wt% mercury, 0.31–2.50 wt% boron, and 0.0625–0.500 wt% cadmium, respectively. An excellent agreement has been observed between the calculated and experimental yields of the gamma rays. Also minimum detection limit (MDC) of the CeBr3 detector was measured for boron, cadmium and mercury samples. The CeBr₃ detector has 23% smaller value of MDC_B and 18% larger value of MDC_Cd than those of a LaBr₃:Ce detector of equivalent size.

This study has shown that CeBr₃ detector has an excellent response for the low energy prompt gamma-rays with almost an order of magnitude low intrinsic activity as compared to LaCl₃:Ce and LaBr₃:Ce detectors of equivalent volume.

1. Introduction

The problems associated with higher intrinsic activities of high resolution LaBr₃:Ce, detectors has led to the development of low intrinsic activity cerium tribromide (CeBr₃) gamma ray detectors (Guss et al., 2010; Quarati et al., 2013; Drozdowski et al., 2008). CeBr₃ detectors have comparable properties as compared to LaBr₃: Ce and LaCl₃:Ce detectors but have less intrinsic activity than the lanthanum halide detectors (Guss et al., 2014). The major part of the intrinsic activity of a CeBr₃ detector arises mainly due to

impurity of [227]Ac in detector raw material has an energy spectrum spread over 1200–2200 keV energy range [Quarati et al., 2013]. Although the CeBr₃ detector has 1.33 times lower alpha/gamma ratio as compared to the LaBr₃:Ce detector (Guss et al., 2010), it has a poorer energy resolution of 4.1% for 661 keV as compared to 2.9% reported for a LaBr₃:Ce detector of equivalent size. The main reason for the poorer energy resolution of the CeBr₃ detector is due to optical self-absorption of radiation caused by excessive cerium contents in the CeBr₃ detector material (Ter Weele et al., 2014; Dorenbos, 2002; Quarati et al., 2014). Due to its lower intrinsic activity, the Ce:Br₃ detector has one-order of magnitude larger detection efficiency around 1461 and 2641.5 keV energies as compared to the LaBr₃:Ce detector (Quarati et al., 2013). This offers excellent opportunities for the application of the CeBr₃ detector in

the detection of ^{40}K and ^{208}Tl(^{232}Th) in environmental samples (Quarati et al., 2013). Furthermore, the lower intrinsic activity of CeBr$_3$ detectors may improve the signal to noise ratio in gamma ray spectra and hence offer better performance in prompt gamma ray applications as compared to LaBr$_3$:Ce and LaCl$_3$:Ce detectors (Chichester et al., 2007; Guss et al., 2010).

A cylindrical 76 mm × 76 mm (height × diameter) Ce:Br$_3$ detector has been acquired from Scionix Holland BV, The Netherlands for the prompt gamma neutron activation analysis program at King Fahd University of Petroleum and Minerals (KFUM), Dhahran, Saudi Arabia. The detector has an energy resolution of 4.4% for 661 keV gamma rays from ^{137}Cs source. The performance of the Ce:Br$_3$ detector was tested for low energy prompt gamma-rays following the procedure used for previous performance tests of the KFUPM LaBr$_3$:Ce (Naqvi et al., 2015, 2011) and LaCl$_3$:Ce (Naqvi et al., 2012a) detectors. The CeBr$_3$ detector tests were carried out using a previously designed portable neutron generator-based PGNAA setup (Naqvi et al., 2015). The findings of this study are reported in this paper.

2. Intrinsic activity measurements of Ce:Br$_3$ detector

Ideally, the CeBr3 detector should be free of intrinsic activity because Ce and Br are both non-radioactive. However, it has an intrinsic activity due to ^{227}Ac impurity in the detector material. The intrinsic activity the of CeBr$_3$ detector was measured following the procedure used previously for intrinsic activity measurements of LaCl$_3$:Ce (Naqvi et al., 2012a) and LaBr$_3$:Ce detectors (Naqvi et al., 2012b). Detector intrinsic activity was measured directly when it was installed in the PGNAA setup without any additional low background chamber to isolate detector intrinsic activity from room background. For continuity sake it will be briefly described here. The detector signal, which was routed through a pre-amplifier, was processed through a spectroscopy amplifier with shaping time of 1 μs. The amplifier signal was processed by a Multichannel Buffer (ADC) for subsequent storage in a personal computer. Fig. 1 shows the detector intrinsic activity pulse height spectrum superimposed upon the detector energy calibration spectrum taken with a ^{207}Bi gamma ray source. The detector intrinsic activity spectrum without ^{207}Bi source shows low gamma
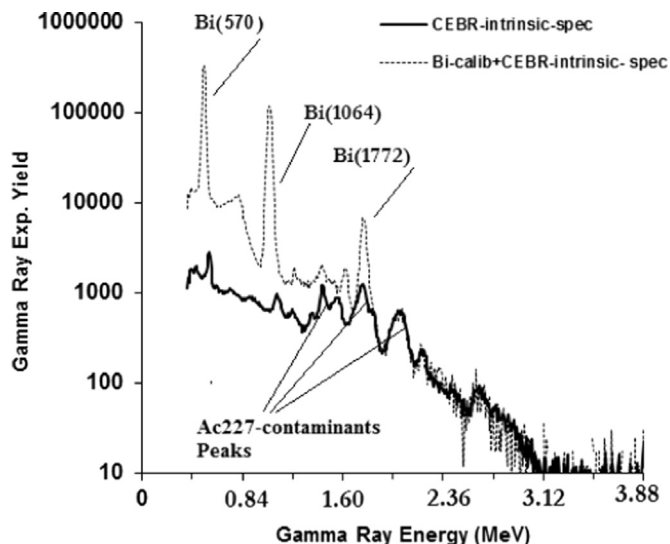

Fig. 1. CeBr$_3$ detector pulse height spectrum taken with ^{207}Bi source superimposed upon pure intrinsic activity spectrum exhibiting three gamma ray peaks of ^{207}Bi along with detector intrinsic activity peaks due to ^{227}Ac contamination.
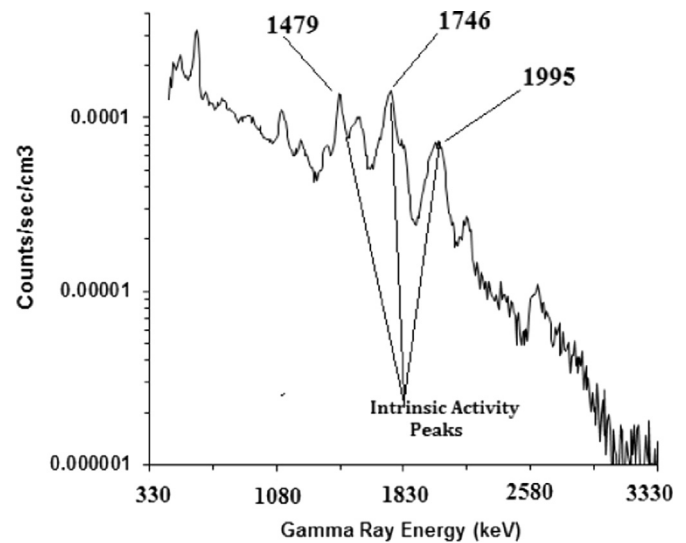

Fig. 2. CeBr$_3$ detector total intrinsic activity pulse height spectrum plotted in units of counts/s/cm^3 as a function of gamma ray energy.

ray background below 1.4 MeV energy. The gamma ray intrinsic activity spectrum of the detector over 1200–2200 keV energy range is due to gamma rays emitted by the alpha emitter contaminants of ^{227}Ac impurity produced by alpha particles of energies 5716 keV (^{223}Ra); 6000 keV (^{227}Th); 6623 keV (^{211}Bi); 6819 keV (^{219}Rn); 7386 keV (^{215}Po) (Quarati et al., 2013).

Fig. 2 shows the intrinsic activity spectrum the CeBr$_3$ detector in units of counts/s/cm^3 as a function of gamma ray energy, which was used to calculate the intrinsic activity rate per unit volume of the CeBr$_3$ detector. Fig. 2 also shows three prominent peaks of intrinsic activity due to radioactive decay of ^{227}Ac impurity contaminants corresponding to 1479, 1746 and 2000 keV (Quarati et al., 2013). In the present study the CeBr$_3$ detector intrinsic activity was measured over two different energy ranges, namely the total intrinsic activity was measured over 0.33–3.33 MeV energy range (called total intrinsic activity in the following paragraphs) while the ^{227}Ac activity (called partial ^{227}Ac activity in the following paragraphs) was measured over 1.20–2.20 MeV range. The total activity of the CeBr$_3$ detector was measured to be 0.022 ± 0.001 counts/s/cm^3 while the partial ^{227}Ac activity was measured to be 0.007 ± 0.001 counts/s/cm^3. Previously, the intrinsic activities of two smaller 50 mm x 50 mm cylindrical CeBr$_3$ detectors, namely detector # SBX 431 and detector # SFB 308, have been measured (Quarati et al., 2013). For the SBX 431 detector they reported a total activity of 0.019 ± 0.001 counts/s/cm^3 and a partial ^{227}Ac activity of 0.001 ± 0.0005 counts/s/cm^3. For the SFB 308 detector the total activity was reported to be 0.043 ± 0.001 counts/s/cm^3 while the partial ^{227}Ac activity was 0.022 ± 0.001 counts/s/cm^3. The partial ^{227}Ac activity of the KFUPM CeBr$_3$ detector is 85% higher than that of the SBX 431 detector while it is 3.1 times less than that of the SFB 308 detector. This intrinsic activity variation may be due to different ^{227}Ac contaminants in the CeBr$_3$ detector crystals used (Quarati et al., 2013).

Previously, the intrinsic activity rate of the cylindrical LaBr$_3$:Ce (Naqvi et al., 2012b) and LaCl$_3$:Ce detectors (Naqvi et al., 2012a) were determined from the 1468 keV peak activity. The intrinsic activity-rate of the LaCl$_3$:Ce detector was measured to be 0.157 counts/s/cm^3 while for the LaBr$_3$:Ce detector it was measured to be 0.182 counts/s/cm^3. Compared to the intrinsic activities of LaCl$_3$:Ce and LaBr$_3$:Ce detectors, the total activity of the CeBr$_3$ detector (used in the present study) is 7 and 8 times less than those of the LaCl$_3$:Ce (Naqvi et al., 2012a) and LaBr$_3$:Ce detectors (Naqvi et al., 2012b), respectively.

3. Prompt gamma ray measurements using Ce:Br₃ detector

The performance of the 76 mm × 76 mm CeBr₃ detector was tested through prompt gamma-ray yield from mercury, cadmium and boron-contaminated water samples following the procedure described earlier for a large 100 mm × 100 mm LaBr₃:Ce detector (Naqvi et al., 2015). For continuity's sake it will be described briefly here. The portable neutron generator-based PGNAA setup consists of a cylindrical moderator made of high density polyethylene. The moderator has a central cylindrical cavity that can accommodate a cylindrical specimen with a maximum diameter of 9 cm and a length of 14 cm. A cylindrical 76 mm × 76 mm (diameter × length) CeBr₃ gamma-ray detector, with its longitudinal axis aligned along the moderator and sample's major axis, views the sample at a right angle to the neutron generator axis. Fig. 3 shows the PGNAA setup with the high density polyethylene cylindrical moderator, portable neutron generator and the CeBr₃ detector. In order to prevent undesired gamma-rays and neutrons from reaching the detector, lead and paraffin shielding were provided around the gamma-ray detector.

3.1. Measurement of CeBr₃ detector activation spectrum

The activation spectrum of the CeBr₃ detector was measured using the portable neutron generator based PGNAA setup described in Section 3. The activation spectrum of the CeBr₃ detector was recorded for 20 min runs using a pure water sample. A pulsed beam of 2.5 MeV neutrons was produced via the D(d,n) reaction using a 70 µA deuteron beam of 70 keV energy. The deuteron pulse had a width of 800 micro seconds and a frequency of 250 Hz. The activation spectrum of the CeBr₃ detector contains prompt gamma-ray peaks due to the capture of thermal neutrons in Br and Ce elements present in the Ce:Br₃ detector material along with small intrinsic activity peaks due to ^{227}Ac contamination. The energies and intensities of prominent prompt gamma-rays due to the capture of thermal neutrons in cerium and bromine are listed in Table 1 (Choi et al., 2006). Most of these peaks are observed in the sample background spectra taken with our CeBr₃ detector. The sample background spectrum must be subtracted from the sample spectrum to obtain background free prompt gamma ray spectrum of the sample.

The activation spectrum of the CeBr₃ detector, shown in Fig. 4, contains the prompt gamma-ray lines of bromine and cerium along with the 2.22 MeV hydrogen capture peak of thermal neutrons in the moderator. For comparison's sake, the activation spectrum of a 76 mm × 76 mm LaBr3:Ce detector (Naqvi et al., 2011) is shown in Fig. 5. As compared to Fig. 5, Fig. 4 shows a less complicated activation spectrum of the CeBr3 detector as compared to that of the LaBr3:Ce detector due to missing lanthanum peaks.
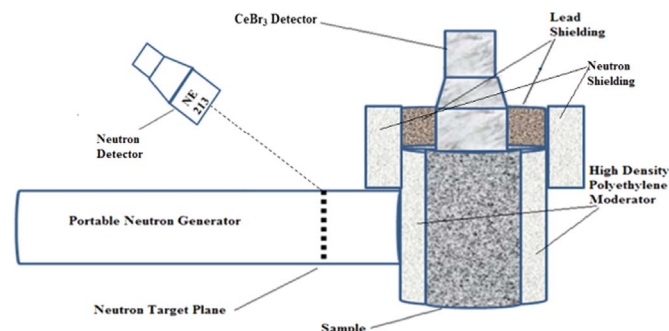

Fig. 3. Schematic representation of the MP320 portable neutron generator used to measure the prompt gamma-ray yield.

Table 1
Energies and partial elemental cross section $\sigma_\gamma{}^z(E_\gamma)$-barns of prominent capture gamma-rays of boron, mercury and cadmium (Choi et al., 2006).

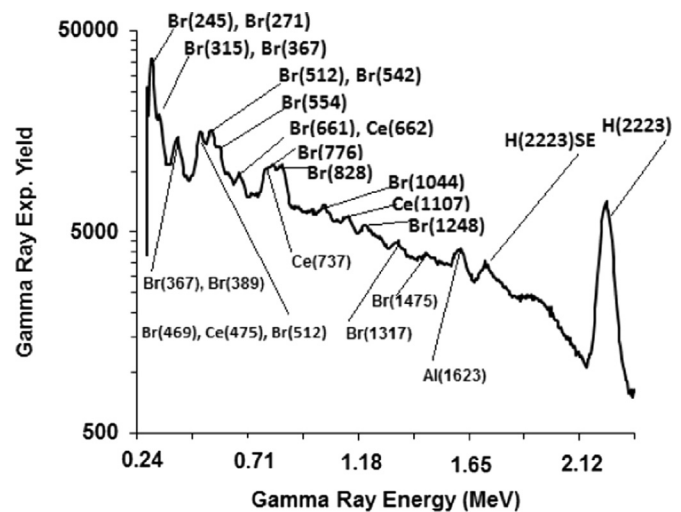| Chemical compound	Element	Gamma-ray energy (keV)	$\sigma_\gamma{}^z$ (E$_\gamma$)-barns
Boric Acid	B(n,α)	478	716
Mercuric nitrate	Hg	368	251
Cerium tri bromide	Br	197	0.434
		245	0.80
		271	0.462
		288	0.253
		367	0.233
		389	0.049
		469	0.29
		512	0.21
		542	0.114
		554*	0.838
		616*	0.39
		619*	0.515
		661	0.082
		776*	0.990
		828*	0.285
		1044*	0.323
		1248*	0.053
		1317*	0.314
		1475*	0.193
Aluminum	Al	1623	0.0099
Cadmium acetate	Cd	245	274
		558	1860
		651	359
Cerium tri bromide	Ce	475	0.082
		662	0.241
		737	0.026
		1107	0.040

* Delayed.

Fig. 4. Prompt gamma-ray spectrum due to activation of the CeBr₃ detector caused by capture of thermal neutrons in Br and Ce elements present in CeBr₃ detector along with hydrogen capture peak from the moderator.

3.2. Prompt gamma-ray measurements of mercury, boron and cadmium contaminated water samples

The prompt gamma-ray analysis of mercury-, boron-, and cadmium-contaminated water samples was carried out using the CeBr₃ detector. Mercury, boron and cadmium were thoroughly mixed with pure water and thereafter poured in cylindrical plastic bottles with 140 mm length and 90 mm internal diameter. Three mercury samples with 0.75, 1.25 and 2.5 wt% mercury concentration, three boron samples with 0.031, 0.125, and 0.250 wt% boron concentrations, and three cadmium samples with 0.0625, 0.125 and 0.25 wt% cadmium concentration were prepared. The
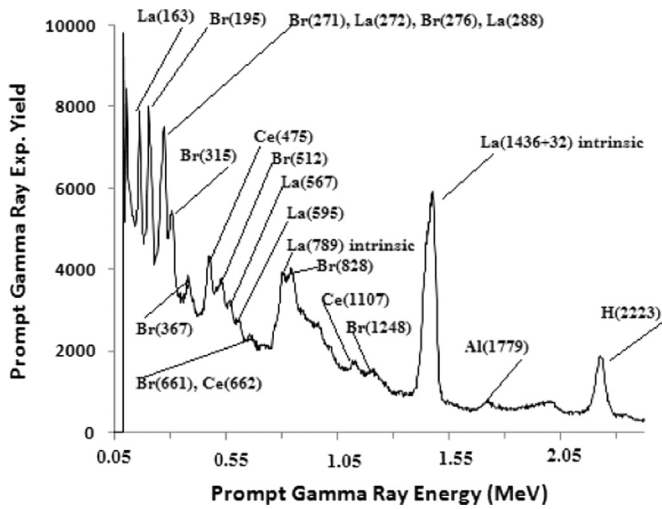
Fig. 5. Prompt gamma-ray spectrum due to activation of a 76 mm × 76 mm LaBr$_3$: Ce detector caused by capture of thermal neutrons in La, Br and Ce elements present in the LaBr$_3$:Ce detector along with hydrogen capture peak from the moderator (Naqvi et al., 2011).

Fig. 6. Enlarged prompt gamma-ray experimental pulse height spectra of boron, mercury and cadmium contaminated water samples superimposed upon background spectrum taken with pure water sample, showing location of boron, mercury and cadmium peaks and their interference with detector activation peaks.
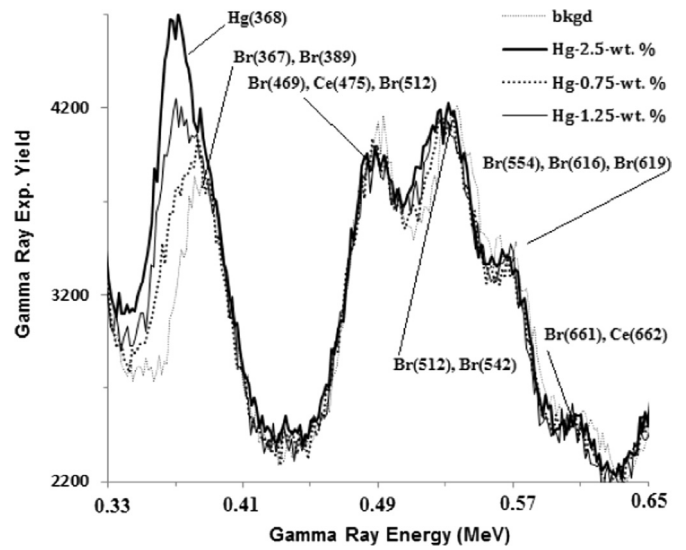

Fig. 7. Prompt gamma-rays pulse height spectra of three mercury contaminated water samples containing 0.75, 1.25 and 2.50 wt% mercury superimposed upon background spectrum taken with pure water.
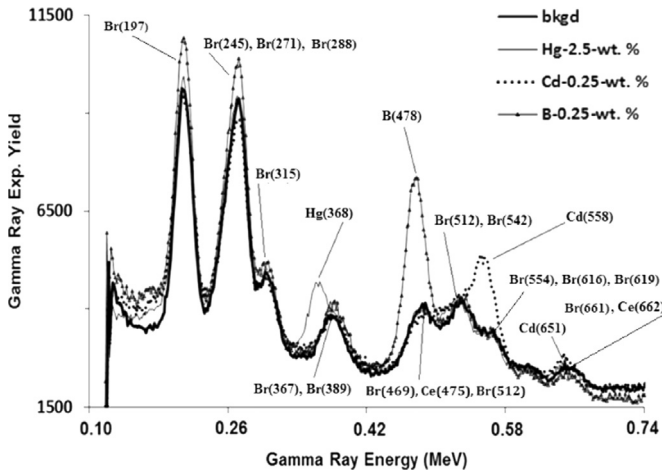
cadmium superimposed upon background spectrum. The Hg(368), B(478) and Cd(558) peaks are quite prominent. Fig. 6 also shows interference of mercury, boron and cadmium prompt gamma ray peaks with detector activation peaks.

Due to finite energy resolution of the detector, the energy of centroid of resultant peak of unresolved interfering peaks is given by cross section-weighted average energy of the peaks. For Br(367) and Br(389) peaks, the resultant peak centroid energy is 378 keV, which was verified experimentally. Similarly for Br(469), Ce(475) and Br(512) peaks, cross section-weighted energy of resultant peak centroid is 486 keV. The cross section-weighted centroid energy of Br(512) and Br(542) interfering peaks is 522 keV. The cross section-weighted centroid energy of Br(554), Br(616) and Br (619) interfering peaks is 576 keV. All resultant peak centroid energies have been verified experimentally.

Fig. 7 and 8 show the pulse height spectra of prompt gamma-rays from water samples containing 0.75, 1.25 and 2.5 wt% mercury superimposed upon each other along with beam associated-
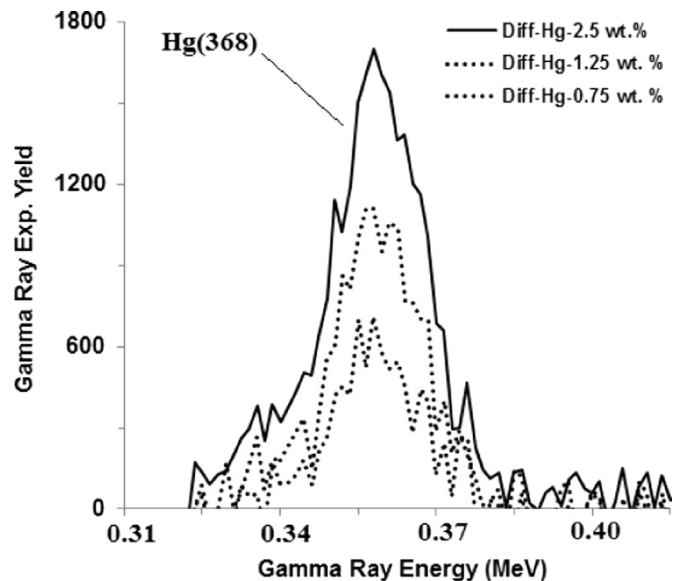
concentrations of mercury, boron and cadmium in water samples were independently measured in the Department of Chemistry, King Fahd University of Petroleum and Minerals, Dhahran, Saudi Arabia using chemical methods such as Atomic Absorption Spectrometry. The water samples were then irradiated in the newly designed PGNAA setup based around MP320 generator (Naqvi et al., 2015). The pulsed neutron beam was produced using the pulsed deuteron beam with specifications given under Section 3.1. Using a pulsed neutron beam in the PGNAA studies, improves the signal to background ratio because beam associated background is reduced and is produced only during beam pulse duration. The prompt gamma-ray data from mercury, boron and cadmium in the contaminated water samples were acquired for a preset time using the Multichannel Buffer based data acquisition system. The data collection time for mercury, boron and cadmium samples typical varies from 20 to 30 min. The neutron flux was monitored during each run using a cylindrical NE213 detector with pulse shape discrimination. The neutron monitor spectrum was further used for neutron flux normalization during data correction. Fig. 6 shows the pulse height spectra of prompt gamma-rays from water samples containing 2.5 wt% mercury, 0.25 wt% boron and 0.25 wt%

Fig. 8. Enlarged prompt gamma-ray pulse height spectra of water samples containing 0.75, 1.25 and 2.50 wt% mercury after background subtraction.
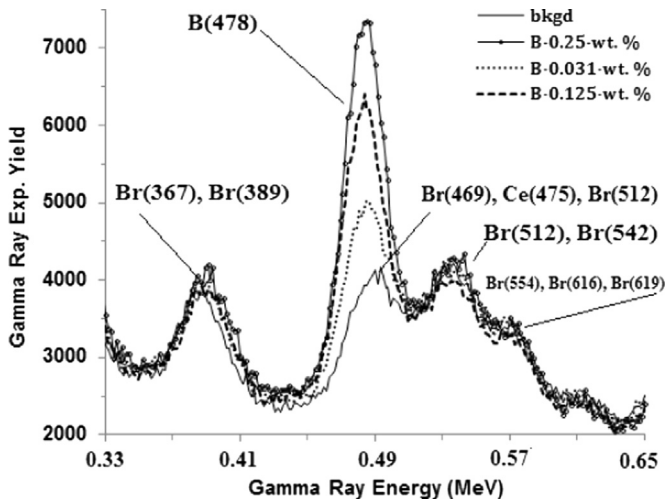
Fig. 9. Prompt gamma-rays pulse height spectra of three boron contaminated water samples containing 0.031, 0.125 and 0.250 wt% boron superimposed upon background spectrum taken with pure water.

Fig. 11. Prompt gamma-rays pulse height spectra of three cadmium contaminated water samples containing 0.0625, 0.125 and 0.250 wt% cadmium superimposed upon background spectrum taken with pure water.

background spectrum taken with pure water sample. In order to show the effect of increasing concentration of mercury on the pulse height spectrum, the pulse height spectra for different mercury concentrations are plotted over 0.32–0.64 MeV. Fig. 7 shows the 368 keV mercury peak interference with 367 and 389 keV peaks from the activation of bromine in the CeBr$_3$ detector. Since mercury peaks contain the contribution of Br(367) and Br(389) peaks, difference spectra of mercury peaks for 0.75, 1.25 and 2.5 wt% concentrations were generated by subtracting the background spectrum from each of them. Fig. 8 shows the enlarged difference spectra of boron peaks for 0.75, 1.25 and 2.5 wt% mercury concentrations.

Figs. 9 and 10 show the pulse height spectra of prompt gamma-rays from water samples containing 0.031, 0.125, and 0.25 wt% boron superimposed upon each other along with beam associated background spectrum taken with pure water sample. In order to show the effect of increasing concentration of boron on the pulse height spectrum, the pulse height spectra for different boron concentrations are plotted over 0.32–0.64 MeV energies. Fig. 9 shows the 478 keV boron peak interference with the Br(469), Ce
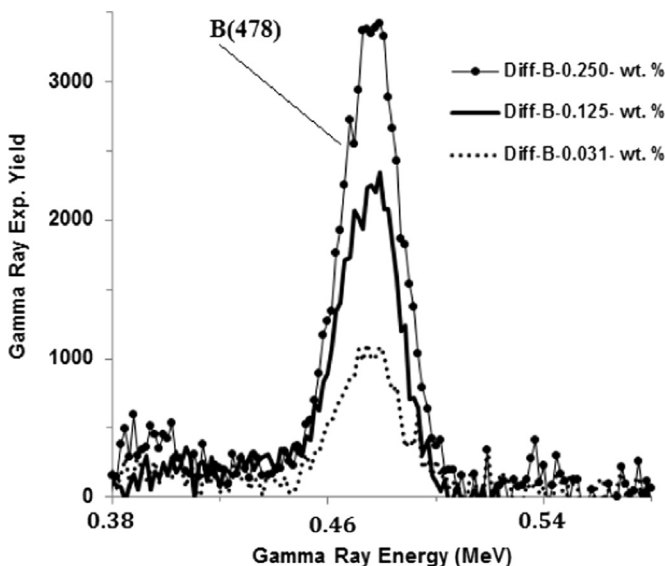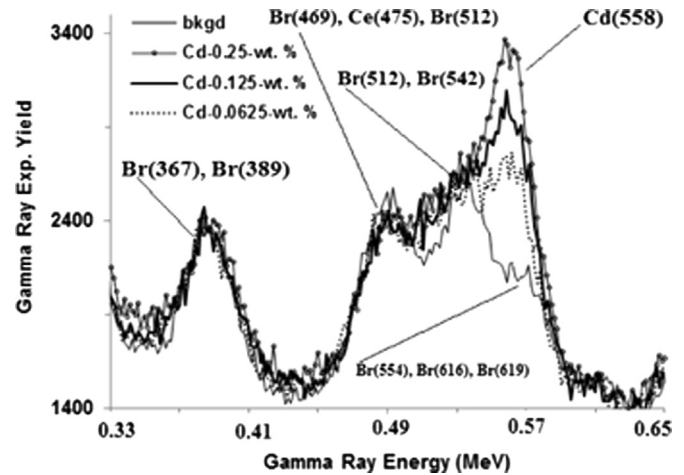
(475) and Br(512) peaks from the activation of the CeBr$_3$ detector. Since boron peaks contain the contribution of Br(469), Ce(475) and Br(512) peaks, the difference spectra of boron peaks for 0.031, 0.12 and 0.25 wt% concentrations were generated by subtracting the background spectrum from each of them. Fig. 10 shows the enlarged difference spectra of boron peaks for 0.031, 0.125, and 0.25 wt% boron concentrations.

Figs. 11 and 12 show the pulse height spectra of prompt gamma rays from water samples containing 0.0625, 0.125 and 0.25 wt% cadmium superimposed upon each other along with the background spectrum taken without sample. In order to show the effect of increasing concentration of cadmium on the pulse height spectrum, the pulse height spectra for different cadmium concentrations are plotted over 0.32–0.64 MeV energies. Fig. 11 shows the 558 keV cadmium peak interference with the 554, 616 and 619 keV peaks from the activation of bromine in CeBr$_3$ detector. Since the cadmium peak contains the contribution of bromine peaks, the difference spectra of cadmium peaks for 0.0625, 0.125 and 0.25 wt% concentrations were generated by subtracting the background spectrum from each of them. Fig. 12 shows the enlarged difference spectra of cadmium peaks for 0.0625, 0.125 and 0.25 wt% cadmium concentration.

Fig. 10. Enlarged prompt gamma-ray pulse height spectra of water samples containing 0.031, 0.125 and 0.250 wt% boron after background subtraction..
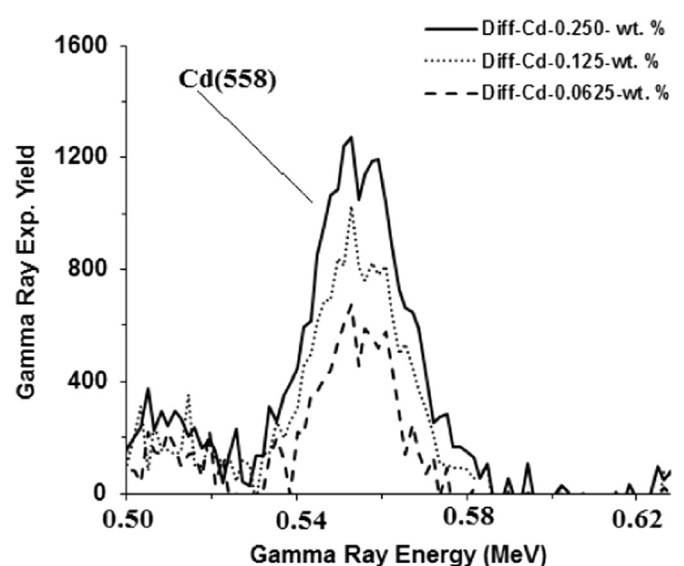

Fig. 12. Enlarged prompt gamma-ray pulse height spectra of water samples containing 0.0625, 0.125 and 0.250 wt% cadmium after background subtraction.
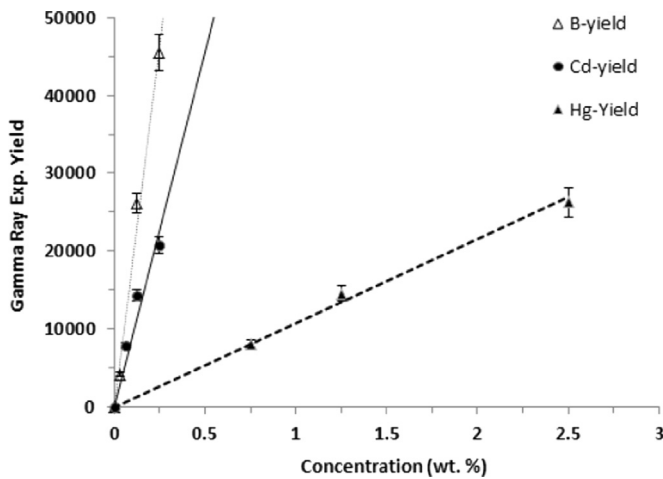
Fig. 13. Integrated yield of Hg((368), B(478) and Cd (558) keV prompt gamma-rays from mercury, boron and cadmium contaminated water samples plotted as a function of mercury, boron and cadmium concentration respectively. The solid line shows normalized-calculated yield of the gamma-rays obtained through Monte Carlo calculations.

Table 2
Coefficient of fit of type gamma ray yield$=b^{*}$con$_{cl}$ (wt%) to gamma ray yield vs concentration data of the B, Hg and Cd samples data.

Sample	b (counts/ wt. % concentration)	uncertainty in b (counts/ wt. % concentration)
Hg	10,068	101
Cd	91,696	781
B	189,224	978

Finally, the integrated yield of boron, mercury, and cadmium gamma ray spectra were calculated by integrating the difference spectra peaks. The integrated yield data was normalized to the same neutron flux and data acquisition time. Fig. 13 shows the integrated yield from difference spectra of boron-, cadmium-, and mercury-contaminated water samples as a function of boron, cadmium and mercury elemental concentration in these water samples. The lines in Fig. 13 represent results of calculated yield of prompt gamma-ray obtained from Monte Carlo calculations following the procedure described elsewhere (Naqvi et al., 2003). The experimental results and the results of Monte Carlo calculation (as shown by corresponding lines in Fig. 13) are in agreement within experimental uncertainties. Table 2 shows the coefficients of least square theoretical fit (Monte Carlo calculations data) made to gamma ray yield vs sample element concentration data.

3.3. Minimum detection limits of boron, cadmium and mercury in water samples

The minimum detection limit (MDC) of the KFUPM portable neutron generator-based PGNAA setup was determined for the 76 mm × 76 mm CeBr$_3$ detector-based system following the procedure described elsewhere in detail (Naqvi et al., 2012a). For the 90 mm × 140 mm (diameter × height) cylindrical water samples, the measured minimum detection limits MDC and their standard deviations σ_{MDCB} for boron, mercury, and cadmium are listed in Table 2. For comparison's sake, the MDC data of a 76 mm x 76 mm cylindrical LaBr3:Ce detector (Naqvi et al., 2011) has also been included in Table 3.

For the CeBr$_3$ detector, the measured values of the minimum detection limit MDC$_B$ and σ_{MDCB} are 24.4 ppm and 7.43 ppm

Table 3
Minimum detection limit (MDC) of boron, cadmium and mercury in water samples using CeBr$_3$ and LaBr$_3$:Ce (Naqvi et al.; 2011) detector based PGNAA setup.

Element	CeBr$_3$ Detector		LaBr$_3$:Ce Detector (Naqvi et al.; 2011)	
	MDC	σ_{MDC}	MDC	σ_{MDC}
B	24.4 ppm	7.43 ppm	30.1 ppm	9.3 ppm
Cd	95.6 ppm	29.1 ppm	78.3 ppm	23.8 ppm
Hg	0.15 wt%	0.05 wt%	–	–

respectively. Compared to a LaBr3:Ce detector of equivalent volume, the CeBr$_3$ detector has a 23% smaller value of MDC$_B$. This improvement might be due to the absence of lanthanum.

The measured values of the minimum detection limit of cadmium MDC$_{Cd}$ and σ_{MDCCd} are 95.6 ppm and 29.1 ppm, respectively. The value of MDC$_{Cd}$ of the CeBr3 detector is 18% larger than that of a LaBr$_3$:Ce detector. As mentioned earlier, due to the absence of lanthanum, the CeBr$_3$ detector was expected to have improved detection sensitivity for the cadmium detection also. However, unlike the boron peak, which interferes with one Ce(475) peak, the cadmium peak interfere with Br(512) and B(554) peaks. This might explain the deterioration of detection sensitivity of the detector for cadmium.

The measured values of the minimum detection limit of mercury MDC$_{Hg}$ and σ_{MDCHg} are 0.15 wt% and 0.05 wt%, respectively. The detection sensitivity of the detector for the mercury is rather poor due to the complete overlap of Hg(368) peak with Br(367) and Br(389) peaks in the detector background.

4. Conclusions

In this study, the response of a 76 mm × 76 mm CeBr$_3$ detector was tested for the detection of low energy prompt gamma-rays by measuring prompt gamma ray yields from mercury-, boron-, and cadmium- contaminated water samples using a portable neutron generator. In the boron-contaminated water samples, the boron concentrations used were 0.031, 0.125, and 0.250 wt%, while in the cadmium-contaminated water samples the cadmium concentrations used were 0.0625, 0.125, 0.250, and 0.500 wt%. The mercury-contaminated water samples were prepared with mercury concentrations of 0.75, 1.25 and 2.5 wt%.

The minimum detection limit (MDC) of the CeBr3 detector was measured for boron, cadmium and mercury samples. The CeBr3 detector has 23% smaller value of MDC$_B$ and 18% larger value of MDC$_{Cd}$ than those of a LaB$_{r3}$:Ce detector of equivalent size.

In spite of small intrinsic activity, the detector has excellent capabilities to detect mercury, boron and cadmium concentration in bulk samples.

References

Chichester, D.L., Simpson, J.D., Lemchak, M., 2007. Advanced compact accelerator neutron generator technology for active neutron interrogation field work. J. Radioanal. Nucl. Chem. 271, 629–637.

Choi, H.D., Firestone, R.B., Lindstrom, R.M., Molnar, G.L., Mughabghab, S.F., Paviotti-Corcuera, R., Revay Zs, Trkov, A., Zhou, C.M.,, 2006. Database of Prompt Gamma-Rays from Slow Neutron Capture for Elemental Analysis. INTERNATIONAL Atomic Energy AGENCY., VIENNA.

Dorenbos, P., 2002. Light output and energy resolution of Ce^{3+}-doped scintillators. Nucl. Instrum. Methods Phys. Res. Sect. A: Accel. Spectrom. Detect. Assoc. Equip. A486, 208–213. http://dx.doi.org/10.1016/S0168–9002(02)00704.

Drozdowski, W., Dorenbos, P., Bos, A.J.J., Bizarri, G., Owens, A., Quarati, F.G.A., 2008. $CeBr_3$ scintillator development for possible use in space missions. IEEE Trans. Nucl. Sci. 55 (3), 1391–1396. http://dx.doi.org/10.1109/TNS.2007.908579.

Guss, P., Reed, M., Yuan, D., Beller, D., Cutler, M., Contreras, C., Mukhopadhyay, S., Wilde, S., 2014. Size effect on nuclear gamma-ray energy spectra acquired by different-sized $CeBr_3$, $LaBr_3$:Ce, and NaI:Tl gamma-ray **detectors**. Nucl. Technol. 185 (3), 309–321.

Guss, P., Reed, M., Yuan, D, Cutler M., Contreras C., Beller D., 2010. Comparison of $CeBr_3$ with $LaBr_3$:Ce, $LaCl_3$:Ce, and NaI:Tl detectors. In: Proceedings of SPIE 7805, Hard X-Ray, Gamma-Ray, and Neutron Detector Physics XII, 78050L, http://dx.doi.org/10.1117/12.862579.

Naqvi, A.A., Khiari, F.Z., Maslehuddin, M., Gondal, M.A., Al-Amoudi, O.S.B., Ukashat, M.S., Ilyas, A.M., Liadi, F.A., Isab, A.A., Khateeb-urRehman, Raashid, M., Dastageer, M.A., 2015. Pulse height tests of a large diameter fast $LaBr_3$:Ce scintillation detector. Appl. Radiat. Isot. 104, 224–231.

Naqvi, A.A., Al-Anezi, M.S., ZameerKalakada, Al.Matouq, FarisA, Maslehuddin, M., Gondal, M.A., Isab, A.A., Khateeb-ur-Rehman, Dastageer, M., 2012a. Response

tests of a $LaCl_3$:Ce scintillation detector with low energy prompt gamma rays from boron and cadmium. Appl. Radiat. Isot. 70, 882–887.

Naqvi, A.A., Al-Matouq, Fares A., Khiari, F.Z., Isab, A.A., Rehman, Khateeb.-ur., Raashid, M., 2012b. Prompt gamma tests $LaBr_3$:Ce and BGO detectors for detection of hydrogen, carbon oxygen in bulk samples. Nucl. Instrum. Methods Phys. Res. 684, 82–87.

Naqvi, A.A., Al-Anezi, M.S., Kalakada, Zameer, Isab, A.A., Raashid, M., Matouq, Al, Ahmed, Faris, Rehman, Khateeb.-ur., Khiari, F.Z., Garwan, M.A., Al-Amoudi, O.S. B., Maslehuddin, M., 2011. Detection efficiency of low levels of boron and cadmium with a $LaBr_3$:Ce scintillation detector. Nucl. Instrum. Methods Phys. Res. A 665, 74–79.

Naqvi, A.A., Nagadi, M.M., Rehman, Khateeb.-ur., Maslehuddin, M., Kidwai, S., 2003. Monte Carlo simulation of the KFUPM PGNAA facility. Radiat. Phys. Chem. 66, 89–98.

Quarati, F.G.A., Alekhin, M.S., Krämer, K.W., Dorenbos, P., 2014. Co-doping of $CeBr_3$ scintillator detectors for energy resolution enhancement. Nucl. Instrum. Methods Phys. Res. A 735, 655–658.

Quarati, F.G.A., Dorenbos, P., Biezen, J., vander, Owens Alan, Selle, M., Parthier, L., Schotanus, P., 2013. Scintillation and detection characteristics of high-sensitivity $CeBr_3$ gamma-ray spectrometers. Nucl. Instrum. Methods Phys. Res. A 729, 596–604.

Ter Weele, D.N., Schaart, D.R., Dorenbos, P., 2014. The effect of self-absorption on the scintillation properties of Ce^{3+} activated $LaBr_3$ and $CeBr_3$. IEEE Trans. Nucl. Sci. 61 (1), 683–688.